# On the relevant role of solids residence time on their $CO_2$ capture performance in the Calcium Looping technology

Antonio Perejón*[,a,b], Juan Miranda-Pizarro[a,c], Luis A. Pérez-Maqueda[a], Jose Manuel Valverde[c]

[a]Instituto de Ciencia de Materiales de Sevilla (C.S.I.C.-Universidad de Sevilla). C. Américo Vespucio 49, Sevilla 41092. Spain.

[b]Departamento de Química Inorgánica, Facultad de Química, Universidad de Sevilla, Sevilla 41071, Spain.

[c]Faculty of Physics, University of Seville, Avenida Reina Mercedes s/n, 41012 Sevilla, Spain.

## Abstract

The multicycle $CO_2$ capture performance of CaO derived from natural limestone and dolomite has been investigated by means of thermogravimetry under realistic Calcium-Looping conditions, which necessarily involve high $CO_2$ concentration and high temperatures in the calcination stage and fast transitions between the carbonation and calcination stages. Natural dolomite allows reducing the calcination temperature as compared to limestone while high calcination efficiency is maintained. This could help reducing the energy penalty of the CaL process thus further enhancing the industrial competitiveness for the integration of this technology into fossil fuel power plants. Importantly, the $CO_2$ capture capacity of the sorbents is critically affected by the solids residence time in the carbonation and calcination stages within the feasible range in practice. Thus, carbonation/calcination residence times play a critical role on the multicycle $CO_2$ capture performance, which has been generally dismissed in previous studies. A main observation is the enhancement of carbonation in the solid-state diffusion controlled phase, which is against the commonly accepted conception that the only relevant phase in the carbonation stage is the fast reaction-controlled stage on the surface of the solids. Thus, the $CO_2$ capture efficiency may be significantly enhanced by increasing the solids residence time in the carbonator.

**Keywords:** $CO_2$ capture; Calcium Looping; limestone; dolomite; thermogravimetry

*Corresponding author:

antonio.perejon@icmse.csic.es
Instituto de Ciencia de Materiales de Sevilla (C.S.I.C.-Univ. Sevilla).
C. Américo Vespucio 49, Sevilla 41092. Spain

# On the relevant role of solids residence time on their $CO_2$ capture performance in the Calcium Looping technology

Antonio Perejón*[,a,b], Juan Miranda-Pizarro[a,c], Luis A. Pérez-Maqueda[a], Jose Manuel Valverde[c]

[a]Instituto de Ciencia de Materiales de Sevilla (C.S.I.C.-Universidad de Sevilla). C. Américo Vespucio 49, Sevilla 41092. Spain.

[b]Departamento de Química Inorgánica, Facultad de Química, Universidad de Sevilla, Sevilla 41071, Spain.

[c]Faculty of Physics, University of Seville, Avenida Reina Mercedes s/n, 41012 Sevilla, Spain.

## Highlights

- Carbonation/calcination residence times critically affect the $CO_2$ capture performance
- Dolomite derived CaO shows higher $CO_2$ capture capacity as compared to limestone
- Best capture capacity behaviour for dolomite is obtained for short calcination stages
- Solid-state diffusion carbonation is determinant at realistic CaL conditions
- Prolonging the residence time in the carbonator enhances the $CO_2$ capture efficiency

# On the relevant role of solids residence time on their $CO_2$ capture performance in the Calcium Looping technology

## 1. Introduction

The Ca-Looping (CaL) process is at the basis of a recently emerged and potentially viable 2nd generation technology for post-combustion $CO_2$ capture [1-3]. This process, early on proposed by Shimizu et al. in 1999 [4], is based on the reversible carbonation/calcination reaction of CaO, which is carried out in two interconnected fluidized bed reactors [1, 5]. Thus, the combustor effluent gas, with low concentration of $CO_2$ (around 15% vol. [6-7]) and at gas velocities of a few m/s, is used to fluidize a bed of CaO particles in a circulating fluidized bed (CFB) carbonator reactor working at around 650ºC under atmospheric pressure. The equilibrium $CO_2$ concentration at this temperature is acceptably low (around 1% vol.) while the reaction is quick enough to attain high $CO_2$ capture efficiency (about 80-90%) for residence times on the order of a few minutes [8-9]. The carbonated solids are then transported into a second CFB reactor (calciner) operated under high $CO_2$ concentration (between 70% and 90% vol.) at temperatures above 900ºC, which are achieved by means of in-situ oxy-combustion [10-11]. Thus a highly concentrated $CO_2$ gas stream is retrieved from the calciner to be compressed and stored while regeneration of CaO takes place at a sufficiently fast rate for its use in a new cycle. CFBs are operated at atmospheric pressure under the fast fluidization regime, with gas velocities of the order of 5-10 m $s^{-1}$ [12-13]. At such large gas velocities, particle clusters are transported upwards through the middle of the bed cross section and recirculated downwards near the walls. Particle mixing is intensive in both axial and radial directions and quite high gas-solid contacting effectiveness is achieved. Thus, the use of CFB reactors in the CaL process would ensure optimum conditions for heat/mass transfer to attain a high $CO_2$ capture and calcination efficiency for residence times of the solids in the reactors of just a few minutes [8, 14-22].

A main advantage of the CaL process over other $CO_2$ capture technologies is the low cost, wide availability and non-toxicity towards the environment of natural CaO precursors such as natural limestone or dolomite [14, 23-26]. However, the efficiency of the CaL process depends critically on the CaO multicycle capture performance. It is believed that a main inconvenient of the Ca process is the irreversible loss of CaO surface area available for fast carbonation in short residence times due to the

progressive sintering by calcination at high temperature as the number of cycles builds up [27]. The progressive loss of CaO activity in short residence times should be compensated by supplying the calciner with a fresh makeup flow of limestone while a flow of poorly active solids is periodically purged to keep the mass balance. Yet, the necessity of continuously calcining fresh limestone at high temperature by oxy-combustion imposes an important energy penalty to the technology [28]. A possible method for reactivating the sorbent would be to incorporate a recarbonator reactor between the calciner and the carbonator, which would minimize the demand of fresh limestone and heat in the calciner [29-31]. On the other hand, an intense research activity is being carried out on the search for Ca-based materials that would exhibit an enhanced capture performance as compared to limestone derived CaO [14, 20, 32]. Dolomite ($CaMg(CO_3)_2$) is an alternative natural CaO precursor, which is also abundantly available at low price [1, 33-34]. According to several studies, the formation of MgO inert grains at CaL conditions in the decomposition of dolomite would help mitigating the loss of CaO carbonation reactivity [14, 35].

Thermogravimetric analysis (TGA) tests have demonstrated that carbonation of CaO particles proceeds along two well differentiated phases. The first stage consists of a reaction-controlled fast phase on the surface of the particles, which is followed by a slower phase limited by solid-state diffusion of $CO_2$ through the $CaCO_3$ product layer. The fast carbonation phase finishes when a carbonate layer (30–50 nm thick) is developed on the particle's surface [36]. Since $CO_2$ capture is restricted to short residence times under low $CO_2$ partial pressure, it is commonly accepted that most of carbonation would occur in the fast carbonation stage [23, 37]. However, TGA observations reveal that diffusion controlled carbonation is negligible in short residence times only if the sorbent is regenerated under low $CO_2$ partial pressure. This is the case of most TGA tests in which technical limitations do not allow carrying out the calcination stage under a realistically high $CO_2$ concentration atmosphere. In contrast, carbonation in the solid-state diffusion phase is a significant contribution to the overall CaO conversion for carbonation residence times of just a few minutes if calcination is performed under a high $CO_2$ partial pressure [14].

The objective of this work is to investigate the multicycle $CO_2$ capture performance of CaO derived from natural limestone and dolomite as affected by the solids residence times in the calciner and carbonator at CaL conditions. These conditions necessarily involve CaO regeneration by calcination under high $CO_2$ concentration as well as fast

transitions between the carbonation and calcination stages. In most works, calcination conditions used in TGA imply low $CO_2$ partial pressure due to technical difficulties of common furnaces associated to insufficiently high cooling/heating rates (usually around 10ºC/min). This major inconvenience is overcome in our work by using a TG analyzer provided with infrared heating by halogen lamps, which enables cooling/heating rates of up to 300ºC/min. As shown in a previous paper, calcination under high $CO_2$ partial pressure yields a highly sintered sorbent whose capture capacity in the reaction-controlled phase is severely hindered whereas the diffusion-controlled stage is comparatively promoted [35]. Thus, it may be expected that a variation of the residence times within the practically acceptable range of a few minutes has a relevant effect on the multicycle behavior of the sorbent. The main purpose of the present manuscript is to demonstrate the important effect of varying the residence time of the solids in a practical range between 1 and 10 minutes on the multicycle CaO activity. Process simulations using the experimental results presented in this work show that the solids residence time in the carbonator has a relevant influence on the efficiency of $CO_2$ capture especially in the case of dolomite for which solid-state diffusion is enhanced as compared to limestone.

## 2. Materials and methods

The materials employed in this work are natural limestone ($CaCO_3$) of high purity (99.6% $CaCO_3$) provided by Segura S.L. (Matagallar quarry in Pedrera, Sevilla, Spain) and natural dolomite from Bueres (Asturias, Spain). According to X-Ray analyses carried out at room temperature, the predominant phase identified in the dolomite powder is $CaMg(CO_3)_2$ (94.4% wt) with the rest being $CaCO_3$ (~5%) and other impurities (<1%).

Carbonation/calcination (carb/cal) and carbonation/recarbonation/calcination (carb/rec/cal) tests were performed using the thermogravimetric analyzer (TGA) Q5000IR from TA Instruments. This instrument has a high sensitive balance (<0.1 μg) and is equipped with a furnace heated by infrared halogen lamps which allows fast and controlled temperature ramps (300ºC/min). These technical characteristics allow imposing experimental conditions that mimic realistic operating conditions in power plants as regards heating and cooling rates. Heat transfer phenomena is minimized by

placing the sample inside a SiC enclosure heated with the four symmetrically positioned IR halogen lamps, which ensures consistent and uniform heating. Active water-cooling of the surrounding furnace body provides an efficient heat-sink and favors accurate temperature and heating/cooling rate control up to 300ºC/min. The temperature is registered by a thermocouple positioned close to the sample underneath it. Quick heating of the gas up to the desired temperature is achieved by using a small gas flow rate (50 ml/min). At this small flow rate the gas velocity has no influence on the reaction rate.

The experiments consisted of 20 cycles of carbonation/calcination or carbonation/recarbonation/calcination preceded by a calcination of the sample (precalcination stage). Typically, the activity of the CaO derived from limestone regenerated under harsh calcination conditions will decay below 10% after 20 cycles [35]. Thus, the multicycle behavior of the sorbent along this number of cycles as observed in our work yields significant information on the evolution of its capture capacity. The average number of cycles that a particle undergoes in the CaL process in the practical application will depend on the recirculation flow rate of solids between the carbonator and the calciner and the flow rate of fresh limestone introduced into the system that must balance out the flow rate of purged solids [8].

In each test, the sample is introduced in the furnace, starting with a precalcination stage from room temperature to either 900ºC or 950ºC at 300ºC/min, in a 70% $CO_2$/30% air vol/vol atmosphere. Then the temperature is quickly decreased (300ºC/min) to 650ºC to introduce a carbonation stage under a 15% $CO_2$/85% air vol/vol atmosphere for either 1, 5 or 10 minutes. After that, the sample is calcined by quickly increasing the temperature (300ºC/min) to either 900ºC or 950ºC for 1 or 5 minutes under high $CO_2$ concentration (70% $CO_2$/30% air vol/vol). Residence times of 5 minutes for both calcination and carbonation stages have been considered as the reference times. In some of the tests, a recarbonation stage under a 90% $CO_2$/10% air (vol/vol) atmosphere at 800ºC is introduced between the carbonation and the calcination stages.

Post-combustion flue gases typically contains $CO_2$ in a volume concentration of about 10-17% but also ashes and $SO_2$, which may interfere with the carbonation reaction [28]. The presence of $SO_2$ leads to $CaCO_3$ or CaO irreversible sulphation with the consequent loss of active sorbent. In fact, both limestone and dolomite are usually employed to capture $SO_2$ in coal fired plants, and the deactivated sorbents from the CaL process can be employed still for efficient $SO_2$ capture [10, 38]. On the other hand, in

precombustion $CO_2$ capture applications such as sorption enhanced methane steam reforming, the flue gas is generally composed by 15-17 vol.% of $CO_2$ with absence of ashes or $SO_2$ that might enhance further deactivation [39]. In our tests, sorbent deactivation as due to the presence of ashes and $SO_2$ is not considered due to technical limitations but it might play an important role to keep in mind.

Samples of small and fixed mass (~10 mg) were tested in order to avoid undesired effects due to gas diffusion resistance through the sample, which would become relevant in this type of analysis for sample masses above 40 mg [40-41]. The average particle size (volume weighted mean) of the powder is 5 μm for limestone and 30 μm for dolomite (Fig. 1), which was measured using a Malvern Mastersizer 2000 instrument by laser diffractometry of samples dispersed in 2-propanol (according to ISO 14887 for Ca-based materials). The small size of the particles allows us also to neglect intra-particle diffusion resistance effects on the reaction rate that would be relevant only for particles of size larger than about 300 μm [36, 42].

# 3. Experimental results and discussion

## 3.1. $CO_2$ capture capacity

### 3.1.1. Natural limestone

The $CO_2$ capture behavior of natural limestone and dolomite has been studied for diverse residence times in the calcination and carbonation stages with the objective of finding the optimal combination that maximizes the multicycle activity of the sorbent. In order to compare objectively the capture performance of these materials, the parameter used is the capture capacity defined as the ratio between the $CO_2$ captured in the carbonation stage and the mass of sorbent before carbonation is started.

Fig.2 shows thermograms of natural limestone cycled at calcination temperatures of 900ºC and 950ºC, respectively where the time evolution of temperature and sorbent mass are illustrated. Fig.2a displays the thermogram corresponding to residence times of 5 minutes for calcination at 900ºC and 5 minutes for carbonation (5'/5' carb/cal).

As may be seen, calcination is not fully attained in the 4 first cycles for limestone calcined at 900ºC, which prevents a complete regeneration of the sorbent. A similar behavior is observed for different calcination/carbonation times when the calcination temperature is 900ºC. If regeneration of the sorbent does not take place completely, the

$CO_2$ capture capacity remains quite low. Since the CaL process requires a continuous makeup flow of fresh limestone, it is important to work under calcination conditions that allow attaining full decarbonation of fresh limestone from the first cycle in short residence times. We observed that the calcination temperature must be increased up to 950ºC in order to achieve complete regeneration of limestone derived CaO for residence times below 5 minutes (Fig. 2b). At this temperature the mass% after calcination matches the mass% of CaO in limestone (56%) from the first cycle, which means that complete decarbonation takes place and CaO is fully regenerated according to the reaction:

$$CaCO_3 \leftrightarrows CaO + CO_2 \qquad (1)$$

Figure 3 shows results of the capture capacity versus the cycle number (N) for natural limestone and for different residence times in the carbonation/calcination stages (calcination at 900ºC). The sorbent exhibits the highest capture capacity after the first cycle and till the sixth cycle for the test carried out under reference carbonation/calcination times (5'/5' carb/cal), with a capture capacity of 0.09 in the 20$^{th}$ cycle. On the other hand, the highest capture capacity from the ninth cycle is obtained for residence times 10'/1' carb/cal even though in the first 8 cycles at these conditions the sorbent cannot be fully regenerated, which yields a relatively low capture capacity. The sorbent presents a similar behavior for the experiment 5'/1' carb/cal, but with a lower capture capacity as the number of cycles is increased. Capture capacity values are 0.15 and 0.10 for the 20$^{th}$ cycle in the tests 10'/1' and 5'/1' carb/cal, respectively, the latter being similar to the capture capacity obtained for the reference 5'/5' carb/cal conditions. Moreover, it can be appreciated that the sorbent tested under 1'/1' carb/cal presents a similar reactivation to that observed for 10'/1' carb/cal, but exhibits a lower capture capacity after 20 cycles. Even though for N=20 the capture capacity of limestone carbonated for 10 minutes and calcined for 1 minute is enhanced as compared to that obtained for the 5'/1' and 5'/5' carb/cal tests, full regeneration of the sorbent takes place only from the cycle N=9. Thus, the fresh makeup flow of limestone introduced in the calciner would present a poor capture capacity in the first cycles.

The total capture capacity ($T_{CC}$) of the sorbent has been calculated as the sum of the capture capacity in the 20 cycles, in order to compare the amount of $CO_2$ captured for the different residence times studied (Fig. 3). The highest $T_{CC}$ has been obtained for the

reference times of carbonation/calcination, followed by the experiments 10'/1' and 5'/1'.

With the objective of assessing the multicycle behavior of natural limestone when complete calcination takes place from the first cycle, the temperature of this stage was increased up to 950ºC (Fig.4), which is similar to the typical temperature employed in pilot plants and process simulations [10, 28, 43]. The residence times used for the carbonation and calcination stages were 1 and 5 minutes. As may be seen in Fig. 4, the evolution of the capture capacity with the number of cycles differs from that obtained when calcination is performed at 900ºC. For calcination at 950ºC a high capture capacity is achieved from the first cycle due to complete sorbent regeneration even for the case of calcination for just 1 minute. Yet, the capture capacity decreases sharply as the number of cycles increases. Thus, the best performance is observed for the experiment 5'/1' carb/cal in which the sorbent exhibits a high capture capacity in the first cycles although it decays rapidly to about 0.07 at the $20^{th}$ cycle. As compared with the test with the same residence times (5'/1' carb/cal) but with calcination at 900ºC (inset in Fig. 4), the capture capacity is higher for the test with calcination at 950ºC till the cycle number 7 due to incomplete calcination at 900ºC, while from this cycle the capture capacity is higher for the experiment with calcination at 900ºC, arguably due to enhanced sorbent sintering at 950ºC. Moreover, the total capture capacity is markedly higher for the test 5'/1' carb/cal as compared with the other tests.

### 3.1.2. Natural dolomite.

The above study was also performed for natural dolomite, which has been proposed as a potentially advantageous CaO precursor in previous studies to be used for both for $CO_2$ and $SO_2$ capture [14, 44-47]. Recent results suggest that dolomite could be employed as a feasible CaO precursor for the CaL process, needing lower calcination temperatures than limestone, which would reduce the energy penalty of the process. Moreover, the loss of CaO activity is mitigated with the number of cycles for dolomite, which would allow obtaining higher conversion values and improve the durability of the sorbent [14, 48-49].

In the experiments carried out in our work using dolomite, the effect caused by the introduction of a recarbonation stage between carbonation and calcination was also studied (for the first time to our knowledge). Recarbonation consisted of subjecting the material to a high temperature stage under high $CO_2$ concentration (800ºC in 90% $CO_2$

over 3 minutes) with the objective of reactivating it as reported for limestone [18, 30, 50]. According to Li et al. [51-52], the carbonate product grows as islands on the surface of the solid. The increase in temperature during recarbonation would enhance surface diffusion, which favors the formation of higher islands, thus increasing the CaO free surface available for carbonation in a new fast reaction-controlled phase. A possible inconvenient of recarbonation, as observed in our study, is that the subsequent calcination presents a lower decarbonation rate than without the recarbonation stage. Thus, additional energy would be needed in the calciner to attain full calcination. For this reason, we observed also that recarbonation generally does not reactivate the sorbent if the calcination times are too short due to incomplete sorbent regeneration.

When using dolomite calcination was carried out in the present study at 900ºC. Figure 5 presents the thermogram for residence times of 5 minutes for calcination and 5 minutes for carbonation. Complete regeneration of dolomite derived CaO is obtained from the first cycle with faster rates of calcination as compared to limestone, according with the reaction:

$$CaMg(CO_3)_2 \leftrightarrows CaO + MgO + 2CO_2 \qquad (2)$$

It is important to point out that the parameter used to compare the multicycle performance of limestone and dolomite is the capture capacity, which takes into account the possible disadvantage of using dolomite as regards the presence of inert MgO for carbonation at CaL conditions. Despite this fact, natural dolomite exhibits a higher capture capacity than limestone for the reference carbonation/calcination times of 5'/5' carb/cal as demonstrated in a previous work [14].

Data on the sorbent capture capacity as a function of the cycle number for dolomite are presented in Fig.6. The residence times for carbonation and calcination in these tests were 1, 5 and 10 minutes, which are within the practical range for industrial applications [8].

As seen in Fig. 6, the highest long-term capture capacity was observed for carbonation/calcination residence times 5'/1' and 10'/1', followed by 5'/5' carb/cal, with capture capacity values at the 20$^{th}$ cycle of 0.19, 0.17 and 0.14 respectively. On the other hand, a low capture capacity is obtained for the tests with residence times 1'/5' and 1'/1' carb/cal. A further important result is that, for the 5'/1' carb/cal test, full decarbonation of dolomite is obtained at 900ºC in spite of the rather short calcination time of just 1'. Thus, carbonation/calcination residence times of 10'/1' using natural

dolomite could be considered as the most convenient combination to be used in the CaL process leading to an almost stable value of the capture capacity close to 0.2 for N = 20 as seen in Fig. 6a. However, if the total capture capacity parameter is considered, the highest $CO_2$ capture after 20 cycles is obtained for the test 5'/1'. It is worth remarking that much higher $T_{CC}$ values are obtained for dolomite as compared with limestone.

Capture capacity values as a function of the carbonation/calcination cycle number for natural dolomite, with the introduction of the recarbonation stage are shown in Fig.6b, for carbonation/calcination residence times of 5'/5' and 10'/1'. Data are compared with results from the same experiments without the introduction of the recarbonation stage.

As may be seen, the sorbent is reactivated for the reference conditions (5'/5' carb/cal) when the recarbonation stage is introduced, with a gain of capture capacity of about 0.02 after 20 cycles. If the carbonation stage is prolonged to 10 min and calcination is shortened to 1 min, recarbonation has the opposite effect on the capture capacity of dolomitic sorbent. Thus, the values of the capture capacity for N=20 are in this case 0.1 and 0.2 with and without recarbonation, respectively. A notable loss in the efficiency of the material for $CO_2$ capture is therefore obtained when the recarbonation stage is introduced and long stages of carbonation are combined with short stages of calcination, which is also reflected in the correspondingly low $T_{CC}$ values.

## 3.2. CaO conversion.

Let us analyze CaO conversion ($X_N$) from the results obtained under diverse conditions. Conversion is defined as the ratio of CaO mass converted to $CaCO_3$ in each carbonation stage to the CaO mass present in the sorbent before carbonation and gives an idea of the reactivity of the CaO grains towards carbonation. For limestone, conversion is calculated by multiplying the capture capacity by the factor $W_{CaO}/W_{CO_2}$, where $W_{CaO} = 56\ g/mol$ and $W_{CO_2} = 44\ g/mol$ are the molecular weights of CaO and $CO_2$ respectively. In the case of dolomite the capture capacity is multiplied by the factor $(1 + W_{MgO}/W_{CaO})W_{CaO}/W_{CO_2}$ to obtain the CaO conversion, where $W_{MgO} = 40\ g/mol$ is the molecular weight of MgO. Conversion data reported in our work were fitted using the semi-empirical equation [37, 53-54]:

$$X_N = X_r + \frac{X_1}{\mathrm{k(N-1)} + (1 - X_r/X_1)^{-1}};\ (N = 1, 2 \ldots) \qquad (3)$$

where N is the cycle number, $X_1$ is the conversion at the first cycle, $X_r$ is the residual conversion, which would be attained after a very large number of cycles, and $k$ is the deactivation rate constant.

Figure 7 shows experimental data on CaO conversion and best fit curves obtained from Eq. (1). Experimental conditions discussed above as yielding poor $CO_2$ capture performance show as would be expected high deactivation rates ($k$>0.5). High deactivation rates are obtained for the tests with carb/cal residence times 1'/5' and 5'/5' using limestone with calcination at 950ºC, and natural dolomite with calcination at 900ºC. On the other hand, the test with residence times 5'/1' carb/cal for dolomite presents a low deactivation rate (k = 0.263) and a high residual conversion ($X_r$ = 0.252). As may be seen, dolomite exhibits in general substantially higher values of the residual conversion than limestone.

Eq. (1) cannot be used to fit some of the experimental results such as those obtained for dolomite using carb/cal residence times 10'/1'. It may be seen however that in this case (Fig. 7c) CaO conversion takes a rather stable value of ~0.42 after cycle number 12 with a higher value in the precedent cycles. Remarkably, this is notably larger than the residual conversion obtained in our work for limestone (~0.07) using carb/cal residence times 5'/5' (Fig. 5b), which is similar to the residual value reported in previous works at these reference conditions [31, 37].

From the above analysis, it may be concluded that the multicycle capture performance of CaO can be substantially improved by optimizing the solids residence times in the calciner and carbonator within the limitations imposed by practical conditions and using dolomite as natural precursor. In section 3.4 the possible mechanisms responsible for this behavior will be analyzed in further depth.

## 3.3. Scanning Electron Microscopy analysis (SEM).

Scanning electron microscopy (SEM) micrographs were taken for natural limestone and dolomite samples before and after the multicycle tests (using a high-resolution HITACHI S5200 instrument). All the TGA tests were finished with a calcination stage in which the sorbent was regenerated in order to compare the sorbent

microstructure as affected by the type of precursor and conditions used. Micrographs of the natural precursors, raw limestone and dolomite as received are shown in Fig.8. The microstructure of the materials before the multicycle tests is similar for limestone (Figs. 8a and 8c) and dolomite (Figs. 8b and 8d), showing grains of comparable size (~10μm) and low porosity. A certain laminar arrangement and some fractures in the surface of the particles are also appreciated probably arising from grinding of the mineral in the powder production process. On the other hand, cycled samples (Fig. 9) of limestone and dolomite present a clearly differentiable microstructure. The microstructure of cycled dolomite is illustrated in Figs. 9e and 9f showing a clear segregation of CaO and MgO grains. As may be seen, CaO grains appear markedly sintered as due to the multiple calcinations suffered. On the other hand, MgO grains, which remain inert along the cycles, appear less sintered. In regards to the effect of calcination temperature, calcination at 950ºC yields visible fractures in the CaO grains (Figs. 9a and 9b) presumably caused by intense thermal stress during cycling.

For the tests performed under a reduced calcination temperature (900ºC) (Figs. 9c and 9d), fractures in the particles are not observed, and only some fissures (Fig. 9c) and grain boundary sintering can be appreciated (Fig. 9d). It is also clear that the CaO grains are less sintered when limestone is calcined at 900ºC as compared to 950ºC. It must be remarked that the mechanical strength of the sorbent is also a relevant parameter to be taken into account since in the practical application the marked fracture of the grains may lead to the loss of material due to the excessive production of very fine particles generated by attrition, which cannot be captured by the cyclones.

## 3.4. Role of solid-state diffusion controlled carbonation.

Thermogravimetric analyses generally reveal that carbonation proceeds along two well differentiated stages [8, 15]: the first is a fast reaction-controlled (FR) stage whereas the second stage is slow and governed by a solid-state diffusion process (SD). Chemi-sorption of $CO_2$ on the CaO surface takes place in the fast stage until the $CaCO_3$ layer built up reaches an approximate thickness of 50 nm over the surface of CaO grains, which takes place in a short period of time (typically tens of seconds). Then, the $CO_3^{2-}$ and $O^{2-}$ ions must counter-diffuse through the carbonate layer formed in the fast

phase for the remaining CaO in the interior of the particles to react, which slows down further carbonation [55].

Fig.10a shows the time evolution of sorbent mass% during 5 minutes carbonation and calcination stages at the 20$^{th}$ cycle for natural limestone and dolomite (carbonation at 650ºC, 15% $CO_2$/85% air vol/vol, and calcination at 900ºC, 70% $CO_2$/30% air vol/vol).

As can be observed in Fig. 10, the fast carbonation stage is clearly shorter than the diffusion-controlled carbonation stage. Moreover, it can be clearly appreciated the great importance of carbonation by solid-state diffusion for dolomite. In this case, the diffusion controlled stage leads to a capture of $CO_2$ approximately twice the capture attained in the fast reaction-controlled stage for the 5'/5' carb/cal reference conditions. In Fig. 10b, the time evolution of dolomite mass% at the 20$^{th}$ cycle is compared for residence times 10'/1' and 1'/1' carb/cal. As might be expected, it becomes clear that the capture capacity of dolomite is enhanced at prolonged carbonation times due to the diffusion controlled stage.

The relative importance of the fast reaction-controlled and diffusion controlled carbonation stages have been studied in our work by calculating the conversion in each phase at each cycle. Data on conversion in both phases ($X_{FR}$ and $X_{SD}$) for limestone samples carbonated at 650ºC (15% $CO_2$/85% air vol/vol) and calcined at 900ºC (70% $CO_2$/30% air vol/vol) for different residence times are shown in Fig.11.

As can be seen in Fig. 11, conversion in the fast carbonation phase tends towards the same value after 20 cycles regardless of the residence times. On the contrary, a variation of the solid residence time has a significant effect on conversion in the solid-state diffusion controlled phase. Thus, by prolonging the carbonation residence time, substantially higher values of the long-term conversion are obtained. The large value of conversion obtained in the 10'/1' carb/cal test once full regeneration is achieved can be therefore explained from a notable contribution of the solid-state diffusion controlled carbonation. It can be also noticed that conversion in the fast reaction-controlled phase for the experiment 1'/1' carb/cal is higher than for the test 1'/5' carb/cal despite the same carbonation residence time was employed. This result can be explained if we consider that the sorbent would suffer further sintering if the calcination time is increased. Fig.12 shows data on conversion in the fast and diffusion phases for natural limestone samples calcined at 950ºC. The behavior of CaO derived from natural limestone in the fast phase (Fig. 11a) is similar to that observed for calcination at 900ºC (Fig. 12a), with values of $X_{FR}$ in approximately the same range after 10 cycles.

However, a change on the behavior of the sorbent in the diffusion-controlled phase (Fig. 12b) is seen when the carbonation time is modified. The tests with carb/cal residence times 1'/1' and 1'/5' carb/cal show almost the same behavior of $X_{SD}$ with the cycle number, and the experiments with carb/cal residence times 5'/1' and 5'/5' carb/cal show similar and higher conversion values. In this case, the contrast between conversions in both stages is not as marked as when the calcination takes place at 900ºC.

As regards natural dolomite, its behavior shows a relevant dependence on the carbonation residence time as shown in Fig. 13. The relatively higher capture capacity observed for this sorbent as compared to limestone can be explained from the notably large values of conversion in the solid-state diffusion phase as compared to the fast reaction-controlled phase. Solid state diffusion for this CaO precursor plays a more relevant role than for natural limestone, being thus the use of prolonged residence times in the carbonator more critical on the results of the overall conversion.

Data from the experiments using dolomite with and without the introduction of the recarbonation stage are compared in Figs. 13c-d. As can be seen, the introduction of a recarbonation stage hinders diffusive carbonation when the carbonation stage is prolonged up to 10 minutes. A possible explanation to this behavior is that recarbonation enhances crystallinity especially when the degree of carbonation achieved in the previous carbonation stage is high, which hampers solid-state diffusion [17].

## 3.5. Effect of carbonation residence time and sorbent behavior on predicted $CO_2$ capture efficiency

The integration of the CaL process into a coal fired power plant (CFPP) has been recently analyzed taking into account the important contribution of carbonation in the diffusion-controlled phase [8, 56]. In contrast with previous models, which neglected carbonation in this phase, the new integration model predicts that the residence time of the solids in the carbonator plays a relevant role on the $CO_2$ capture efficiency. Fig. 14a shows the CFPP-CaL integration scheme (adapted from [56]). In the carbonator, the CaO particles entering from the calciner react with the flue gas effluent from the coal-fired power plant. The carbonator model is detailed elsewhere [8]. A main feature of the carbonator model is that the particles remain active beyond the fast reaction-controlled carbonation phase. Thus, the average conversion of the particles leaving the carbonator

is obtained from the sum of the average particle conversion in the fast carbonation phase and the average particle conversion in the diffusive phase. Simulations were made for a 505 MWe coal fired power plant using a value of 0.15 for the volumetric fraction of $CO_2$ in the flue gas entering the carbonator and a flow rate $F_{CO2}$ = 0.1 kg $CO_2$/s. The operating carbonator temperature is 650ºC and it works at atmospheric pressure in a circulating fluidized bed regime (CFB) with a gas pressure loss of about 100 mbar, as calculated from the Kunii-Levenspiel model. Moreover, in the simulation, a sulfation capture capacity of 99% is considered.

The $CO_2$ gas stream exiting the carbonator is sent to different heat exchangers with the objective of recovering its sensible heat before being vented into the atmosphere (see Fig. 14a) whereas the post-combustion flue gas is preheated before entering into the carbonator (Fig. 14b) through two heat exchangers. Heat is extracted from the $CO_2$ gas stream exiting the calciner and from the calciner solids purge stream. Electricity is generated from a secondary steam cycle using the heat produced in the exothermic carbonation reaction (178 kJ/mol) and the sensible heat recovered from the streams exiting the calciner. The energy produced in the carbonator and the energy consumption in the calciner is high due to the large flow of solids recirculated between the reactors, which leads to a power production in the secondary steam cycle similar to that produced in the reference power plant as derived in previous integration models [57-58]. Nevertheless, the energy penalty for the integration of the CaL cycle can be substantially reduced if a heat exchanger is inserted between the solids leaving the calciner and the solids entering into it [56].

Simulations show that the energy penalty ranges between 4% and 7% points over the reference plant efficiency, which represents a decrease of energy as compared to the commercial amine scrubbing technology. Energy penalty is further reduced as the solids residence time in the carbonator is increased, due to the lower heat required in the calciner as the recirculation flow rate is decreased. The interested reader is referred to [8, 56] for a detailed description of the new carbonator and CaL-CFPP integration models, which is out of the scope of the present manuscript.

The relationship between the $CO_2$ capture efficiency and the efficiency penalty in the CaL-CFPP integration is quantified by means of the specific energy consumption per kg of $CO_2$ avoided (SPECCA), which is calculated using the following expression [56, 59-60]:

$$SPECCA = 3600\ \frac{\frac{1}{\eta_{plant}} - \frac{1}{\eta_{ref}}}{E_{ref} - E} \qquad (4)$$

Here $E_{ref}$ and E are the emissions ratio (in kg of $CO_2$ per $kWh_e$) whereas $\eta_{ref}$ and $\eta_{plant}$ are the power plant global efficiency before and after the integration, respectively. SPECCA calculations as affected by the multicycle sorbent behavior can be made from the integration model [56], using the experimental results shown in the present manuscript.

SPECCA values calculated from these simulations to achieve a given global $CO_2$ capture efficiency ($E_{CO2}$) of 90% are shown in Fig. 15 as a function of average solids residence time in the carbonator reactor ($\tau = \frac{N_{Ca}}{F_R} = \frac{W_s}{56F_R}$, where $N_{Ca}$ is the number of moles of CaO in the carbonator, $F_R$ is the mole flow rate of CaO entering from the calciner into the carbonator, and $W_s$ is the total solids inventory in the carbonator). As seen in Fig. 15, the amount of energy required per kg of $CO_2$ avoided decreases as the solid residence time increases due to the relevant contribution of the solid-state diffusion controlled carbonation phase to the total capture capacity of the sorbents. As would be also expected from our TGA results, the values of SPECCA at a given carbonator residence time are substantially lower for dolomite as compared to limestone. For example, a value for SPECCA of 3.17 MJ/kg$CO_2$ is obtained for dolomite as compared to 4.19 MJ/kg$CO_2$ for limestone using 10 minutes as solids residence time (Fig. 15). For comparison, the estimated SPECCA for conventional amine scrubbing post-combustion $CO_2$ capture is about 4.5 MJ/kg$CO_2$ [61].

## 4. Conclusions.

In this work, the effect of varying the carbonation/calcination residence times and calcination temperature in the multicycle conversion behavior of CaO derived from natural limestone and dolomite has been analyzed at Ca-Looping (CaL) conditions for $CO_2$ capture. The multicycle $CO_2$ capture performance of these materials has been tested by means of thermogravimetric analysis (TGA) in a furnace that uses infrared heating by halogen lamps. A main advantage of this setup, as compared to TG analyzers used in most previous studies and based upon electrically heated furnaces, is that CaL conditions can be closely mimicked. These involve high temperature (above 900ºC) and

high $CO_2$ concentration in the calcination environment as well as fast transitions between the carbonation and calcination stages.

The results obtained reveal that natural dolomite is a potentially advantageous alternative to natural limestone, which is the currently used CaO precursor in pilot-scale plants. In general, dolomite derived CaO shows a superior $CO_2$ capture capacity and stability along the carbonation/calcination cycles as compared to limestone. For a given carbonation residence time, the best capture capacity results for dolomite are obtained when the calcination stage is reduced. Dolomite attains full calcination in very short residence times (of about 1 minute) at 900ºC, which is a reduction of 30-50ºC in the calcination temperature usually required for limestone to obtain an acceptable calcination efficiency. As shown in the present study, a variation of the carbonation/calcination residence times within the practical range of a few minutes can drastically affect the $CO_2$ capture capacity of the sorbent. Thus, a main novel conclusion of this work is that carbonation/calcination residence times are highly critical for the efficiency of the CaL technology.

The solid-state diffusion controlled carbonation stage plays a critical role on the multicycle CaO conversion behavior at realistic calcination conditions. This result is in contrast with the commonly accepted conception that the only relevant phase in the carbonation stage is the fast reaction-controlled stage, which has been inferred from previous studies whereby calcination was carried out in an environment of low $CO_2$ concentration. Calcination under high $CO_2$ concentration leads to a marked sintering of the regenerated CaO and therefore to a drastic reduction of the surface area available for the fast reaction controlled stage. Conversely, carbonation in the diffusion controlled stage is relatively promoted. Thus, by prolonging the carbonation residence time up to 10 minutes a relatively stable value of the $CO_2$ capture capacity of about 0.2 is achieved after 20 cycles when using natural dolomite (calcinations for 1 minute at 900ºC) whereas the widely accepted value for the residual capture capacity of limestone is just about 0.06.

TGA data shown in this paper have been used in the simulations of a recently proposed CaL coal fired power plant integration model that considers the influence of the solids residence time in the carbonator reactor on the plant global efficiency penalty. The results show a significant reduction in the energy needed to achieve certain $CO_2$ capture efficiency when the solids residence time in the carbonator is prolonged and/or dolomite

is used instead of limestone. In both cases, $CO_2$ capture is promoted by the enhancement of carbonation in the solid-state diffusion controlled carbonation phase.

## 5. Acknowledgements

Financial support by the Spanish Government Agency Ministerio de Economia y Competitividad (contracts CTQ2014-52763-C2-2-R and CTQ2014-52763-C2-1-R) and Andalusian Regional Government (Junta de Andalucia-FEDER contracts FQM-5735 and TEP-7858) is acknowledged. The authors also thank VPPI-US for the AP current contract. The Microscopy, Functional Characterization and X-ray services of the Innovation, Technology and Research Center of the University of Seville (CITIUS) are gratefully acknowledged.

## 6. References.

[1] J. Blamey, E. J. Anthony, J. Wang, P. S. Fennell, Prog. Energ. Combust., 2010, **36**, 260-279.

[2] M. C. Romano, Chem. Eng. Sci., 2012, **69**, 257-269.

[3] M. K. Mondal, H. K. Balsora, P. Varshney, Energy, 2012, **46**, 431-441.

[4] T. Shimizu, T. Hirama, H. Hosoda, K. Kitano, M. Inagaki, K. Tejima, Chem. Eng. Res. Des., 1999, **77**, 62-68.

[5] C. C. Dean, J. Blamey, N. H. Florin, M. J. Al-Jeboori, P. S. Fennell, Chem. Eng. Res. Des., 2011, **89**, 836-855.

[6] V. Manovic, E. J. Anthony, J. Phys. Chem. A, 2010, **114**, 3997-4002.

[7] W. Wang, S. Ramkumar, D. Wong, L.-S. Fan, Fuel, 2012, **92**, 94-106.

[8] C. Ortiz, R. Chacartegui, J. M. Valverde, J. A. Becerra, L. A. Perez-Maqueda, Fuel, 2015, **160**, 328-338.

[9] M. C. Romano, I. Martínez, R. Murillo, B. Arstad, R. Blom, D. C. Ozcan, H. Ahn, S. Brandani, Energy Procedia, 2013, **37**, 142-150.

[10] B. Arias, M. E. Diego, J. C. Abanades, M. Lorenzo, L. Diaz, D. Martinez, J. Alvarez, A. Sanchez-Biezma, Int. J. Greenh. Gas Control, 2013, **18**, 237-245.

[11] I. Martínez, G. Grasa, R. Murillo, B. Arias, J. C. Abanades, Energ. Fuel, 2012, **26**, 1432-1440.

[12] K. Kim, D. Kim, Y. K. Park, K. S. Lee, Int. J. Greenh. Gas Control, 2014, **26**, 135-146.

[13] J. Ylatalo, J. Ritvanen, T. Tynjala, T. Hyppanen, Fuel, 2014, **115**, 329-337.

[14] J. M. Valverde, P. E. Sanchez-Jimenez, L. A. Perez-Maqueda, Appl. Energ., 2015, **138**, 202-215.

[15] J. M. Valverde, P. E. Sanchez-Jimenez, L. A. Perez-Maqueda, Environ. Sci. Technol., 2014, **48**, 9882-9889.

[16] J. M. Valverde, P. E. Sanchez-Jimenez, L. A. Perez-Maqueda, Appl. Energ., 2014, **126**, 161-171.

[17] J. M. Valverde, P. E. Sanchez-Jimenez, L. A. Perez-Maqueda, M. A. S. Quintanilla, J. Perez-Vaquero, Appl. Energ., 2014, **125**, 264-275.

[18] J. M. Valverde, P. E. Sanchez-Jimenez, L. A. Perez-Maqueda, Fuel, 2014, **123**, 79-85.

[19] P. E. Sanchez-Jimenez, J. M. Valverde, L. A. Perez-Maqueda, Fuel, 2014, **127**, 131-140.

[20] P. E. Sanchez-Jimenez, L. A. Perez-Maqueda, J. M. Valverde, Appl. Energ., 2014, **118**, 92-99.

[21] J. M. Valverde, P. E. Sanchez-Jimenez, A. Perejon, L. A. Perez-Maqueda, Energ. Fuel, 2013, **27**, 3373-3384.

[22] R. Naqvi, J. Wolf, O. Bolland, Energy, 2007, **32**, 360-370.

[23] J. C. Abanades, E. J. Anthony, D. Y. Lu, C. Salvador, D. Alvarez, AIChE J., 2004, **50**, 1614-1622.

[24] G. Grasa, B. González, M. Alonso, J. C. Abanades, Energ. Fuel, 2007, **21**, 3560-3562.

[25] C. C. Cormos, Energy, 2014, **78**, 665-673.

[26] Y. Li, C. Zhao, H. Chen, Q. Ren, L. Duan, Energy, 2011, **36**, 1590-1598.

[27] J. M. Valverde, P. E. Sanchez-Jimenez, L. A. Perez-Maqueda, J. Phys. Chem. C, 2015, **119**, 1623-1641.

[28] A. Perejón, L. M. Romeo, Y. Lara, P. Lisbona, A. Martínez, J. M. Valverde, Appl. Energ., 2016, **162**, 787–807.

[29] C. Salvador, D. Lu, E. J. Anthony, J. C. Abanades, Chem. Eng. J., 2003, **96**, 187-195.

[30] B. Arias, G. S. Grasa, M. Alonso, J. C. Abanades, Energy Environ. Sci., 2012, **5**, 7353-7359.

[31] J. M. Valverde, P. E. Sanchez-Jimenez, L. A. Perez-Maqueda, Appl. Energ., 2014, **136**, 347-356.

[32] S. Tian, J. Jiang, F. Yan, K. Li, X. Chen, Environ. Sci. Technol., 2015, **49**, 7464-7472.

[33] A. M. Kierzkowska, R. Pacciani, C. R. Müller, ChemSusChem, 2013, **6**, 1130-1148.

[34] J. M. Valverde, J. Mater. Chem. A, 2013, **1**, 447-468.

[35] J. M. Valverde, A. Perejon, S. Medina, L. Perez-Maqueda, Phys. Chem. Chem. Phys., 2015, **17**, 30162-30176.

[36] G. Grasa, R. Murillo, M. Alonso, J. C. Abanades, AIChE J., 2009, **55**, 1246-1255.

[37] G. S. Grasa, J. C. Abanades, Ind. Eng. Chem. Res., 2006, **45**, 8846-8851.

[38] J. M. Cordero, M. Alonso, B. Arias, J. C. Abanades, Energ. Fuel, 2014, **28**, 1325-1330.

[39] D. P. Harrison, Ind. Eng. Chem. Res., 2008, **47**, 6486-6501.

[40] N. Koga, J. M. Criado, Int. J. Chem. Kinet., 1998, **30**, 737-744.

[41] M. Alonso, Y. A. Criado, J. C. Abanades, G. Grasa, Fuel, 2014, **127**, 52-61.

[42] F. García-Labiano, A. Abad, L. F. de Diego, P. Gayán, J. Adánez, Chem. Eng. Sci., 2002, **57**, 2381-2393.

[43] A. Charitos, N. Rodriguez, C. Hawthorne, M. Alonso, M. Zieba, B. Arias, G. Kopanakis, G. Scheffknecht, J. C. Abanades, Ind. Eng. Chem. Res., 2011, **50**, 9685-9695.

[44] P. Sun, J. R. Grace, C. J. Lim, E. J. Anthony, Energ. Fuel, 2007, **21**, 163-170.

[45] L. F. de Diego, A. Rufas, F. García-Labiano, M. de las Obras-Loscertales, A. Abad, P. Gayán, J. Adánez, Fuel, 2013, **114**, 106-113.

[46] F. García-Labiano, A. Rufas, L. F. de Diego, M. d. l. Obras-Loscertales, P. Gayán, A. Abad, J. Adánez, Fuel, 2011, **90**, 3100-3108.

[47] E. P. O'Neill, D. L. Keairns, W. F. Kittle, Thermochim. Acta, 1976, **14**, 209-220.

[48] A. Silaban, M. Narcida, D. P. Harrison, Chem. Eng. Commun., 1996, **146**, 149-162.

[49] X. Yang, L. Zhao, S. Yang, Y. Xiao, Asia-Pac. J. Chem. Eng., 2013, **8**, 906-915.

[50] G. Grasa, I. Martinez, M. E. Diego, J. C. Abanades, Energ. Fuel, 2014, **28**, 4033-4042.

[51] Z. S. Li, H. M. Sun, N. S. Cai, Energ. Fuel, 2012, **26**, 4607-4616.

[52] Z. S. Li, F. Fang, X. Y. Tang, N. S. Cai, Energ. Fuel, 2012, **26**, 2473-2482.

[53] J. M. Valverde, P. E. Sanchez-Jimenez, A. Perejon, L. A. Perez-Maqueda, Phys. Chem. Chem. Phys., 2013, **15**, 11775-11793.

[54] J. M. Valverde, Chem. Eng. J., 2013, **228**, 1195-1206.

[55] Z. C. Sun, S. W. Luo, P. P. Qi, L. S. Fan, Chem. Eng. Sci., 2012, **81**, 164-168.

[56] C. Ortiz, R. Chacartegui, J. M. Valverde, J. A. Becerra, Appl. Energ., 2016, **169**, 408-420.

[57] A. Martínez, Y. Lara, P. Lisbona, L. M. Romeo, Int. J. Greenh. Gas Control, 2012, **7**, 74-81.

[58] I. Vorrias, K. Atsonios, A. Nikolopoulos, N. Nikolopoulos, P. Grammelis, E. Kakaras, Fuel, 2013, **113**, 826-836.

[59] H. M. Kvamsdal, M. C. Romano, L. van der Ham, D. Bonalumi, P. van Os, E. Goetheer, Int. J. Greenh. Gas Control, 2014, **28**, 343-355.

[60] M. C. Romano, Int. J. Greenh. Gas Control, 2013, **18**, 57-67.

[61] European Benchmarking Task Force. D 4.9, Politecnico di Milano – Alstom UK, 2011

## Figures and Figure Captions

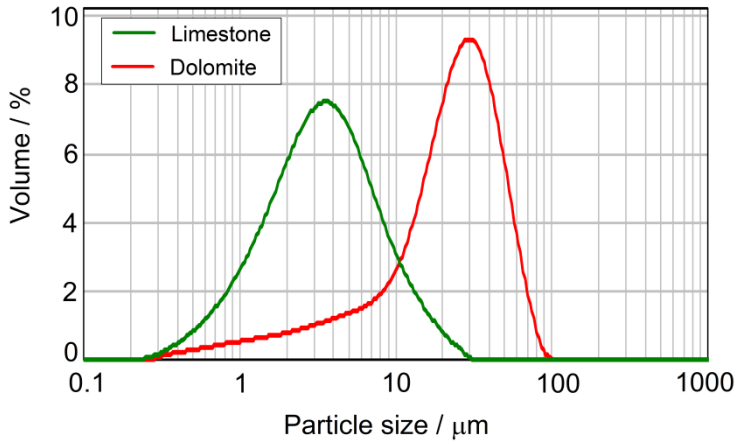


**Fig 1.** Particle size distribution of samples of natural limestone and natural dolomite used in the experiments.

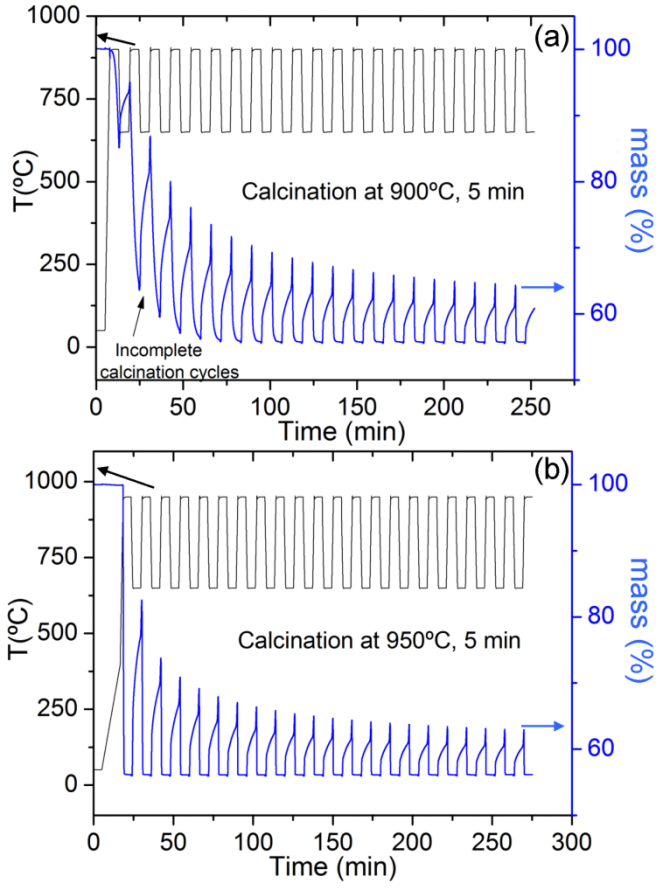


**Fig.2.** Natural limestone thermograms showing the time evolution of temperature and sorbent mass% during calcination/carbonation cycles. (a) Calcination at 900ºC (70% $CO_2$/30% air vol/vol) for 5 minutes and carbonation at 650ºC (15% $CO_2$/85% air vol/vol) for 5 minutes. (b) Calcination at 950ºC (70% $CO_2$/30% air vol/vol) for 5 minutes and carbonation at 650ºC (15% $CO_2$/85% air vol/vol) for 5 minutes.

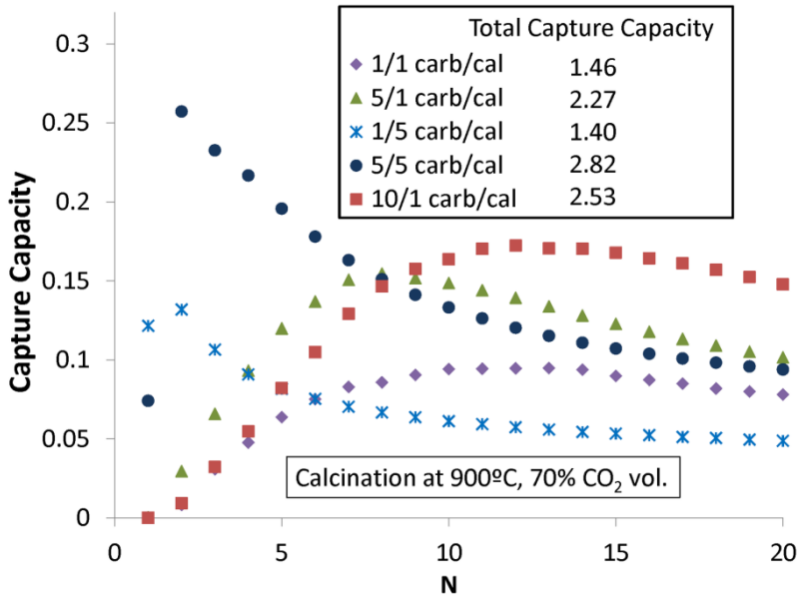


**Fig.3.** Capture capacity versus cycle number (N) for carb/cal tests using natural limestone. Calcination at 900ºC (70% $CO_2$/30% air vol/vol) for 1 or 5 minutes and carbonation at 650ºC (15% $CO_2$/85% air vol/vol) for 1, 5 or 10 minutes as indicated. The total capture capacity ($T_{CC}$) of each test is also indicated.

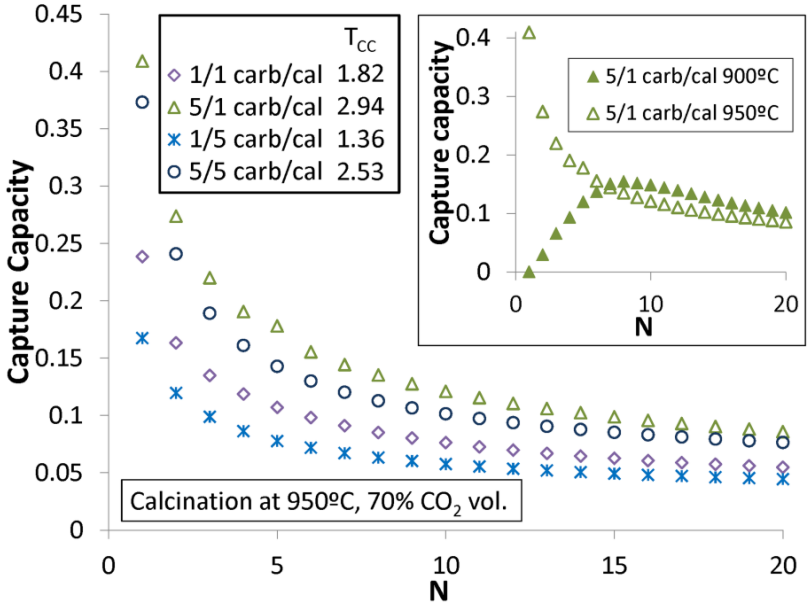


**Fig.4.** Capture capacity as a function of the carbonation/calcination cycle number for natural limestone. Calcination at 950ºC (70% $CO_2$/30% air vol/vol) for 1 and 5 minutes, and carbonation at 650ºC (15% $CO_2$/85% air vol/vol) for 1 and 5 minutes as indicated in the inset. The total capture capacity ($T_{CC}$) of each test is also included. The inset shows a comparison of the tests 5'/1' carb/cal with calcinations at 900ºC and 950ºC.

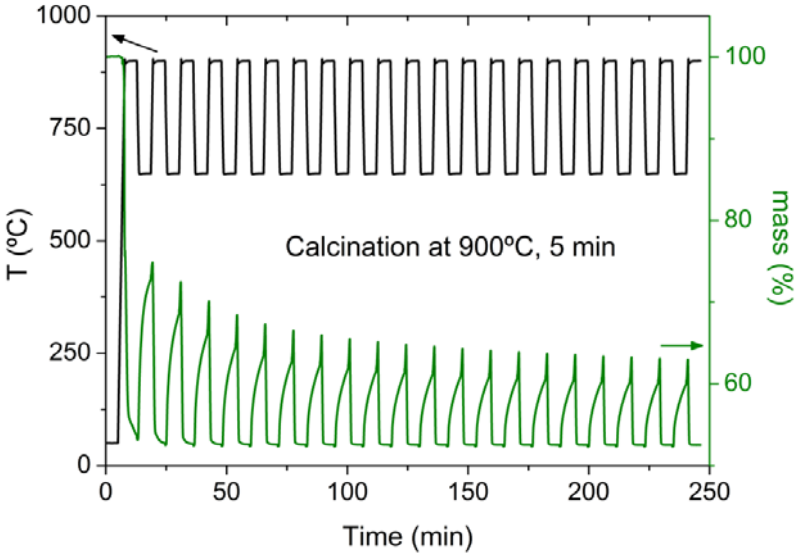


**Fig.5.** Natural dolomite thermogram showing the time evolution of sorbent mass % during calcination/carbonation cycles. Calcination at 900ºC (70% $CO_2$/30% air vol/vol) for 5 minutes and carbonation at 650ºC (15% $CO_2$/85% air vol/vol) for 5 minutes.

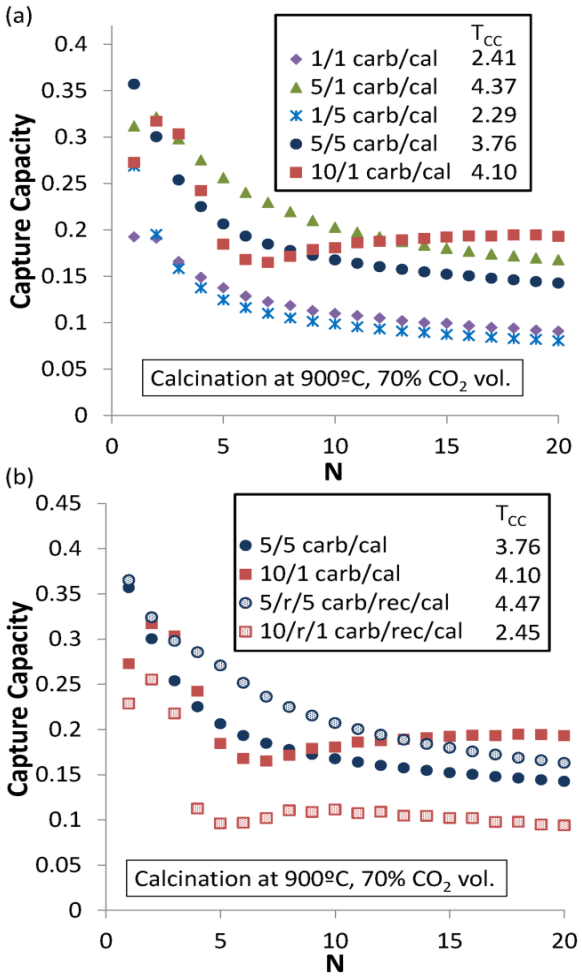


**Fig.6.** Capture capacity versus carbonation/calcination number for natural dolomite. Carbonation at 650ºC (15% $CO_2$/85% air vol/vol) for 1, 5 or 10 minutes, recarbonation at 800ºC (90% $CO_2$/10% air vol/vol) for 3 minutes (in b), and calcination at 900ºC (70% $CO_2$/30% air vol/vol) for 1 or 5 minutes as indicated. The total capture capacity ($T_{CC}$) for each test is indicated in the insets.

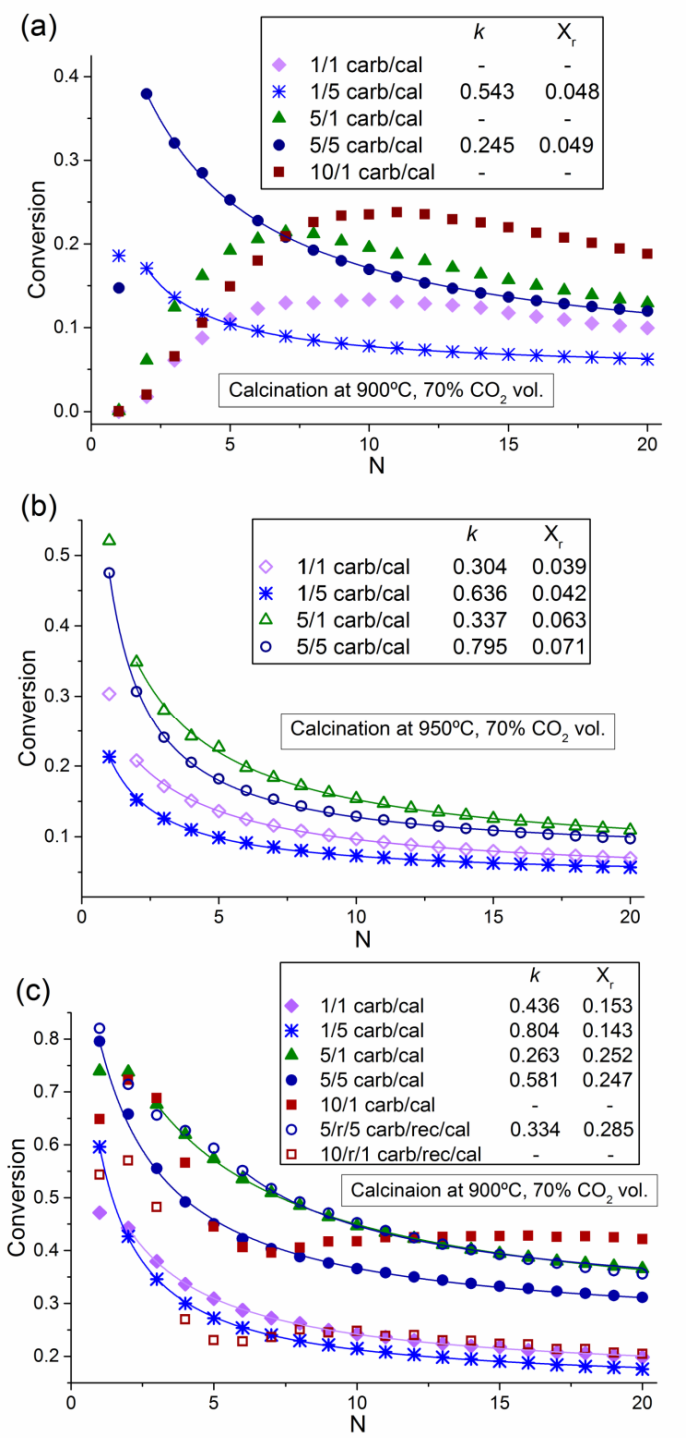


**Fig.7.** Conversion versus the cycle number for natural limestone calcined at 900ºC (a) and 950ºC (b) and natural dolomite calcined at 900ºC (c). The solid lines represent the best fit of equation 1 to the data when the asymptotically behavior starts. In the insets the values of *k* (deactivation constant) and the $X_r$ (residual conversion) are shown.

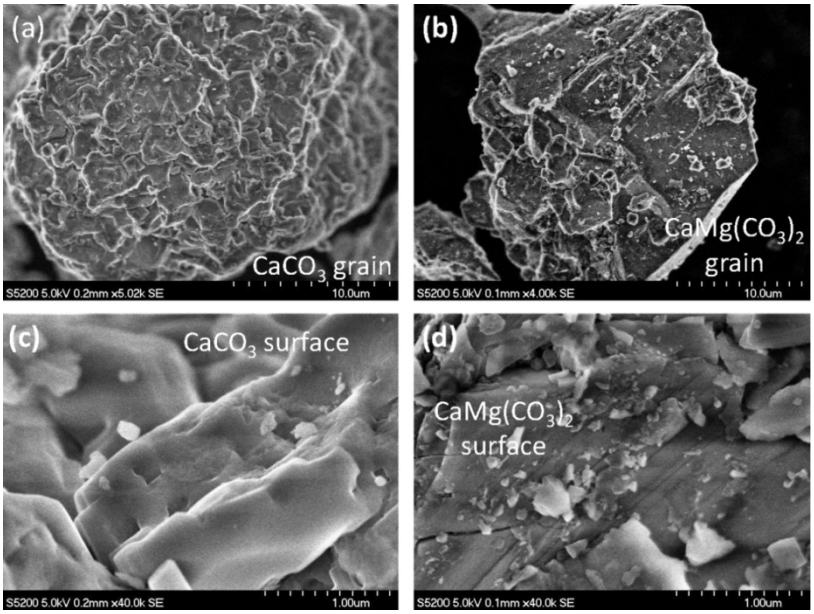


**Fig.8.** SEM micrographs of raw samples of natural limestone (a and c) and dolomite (b and d).

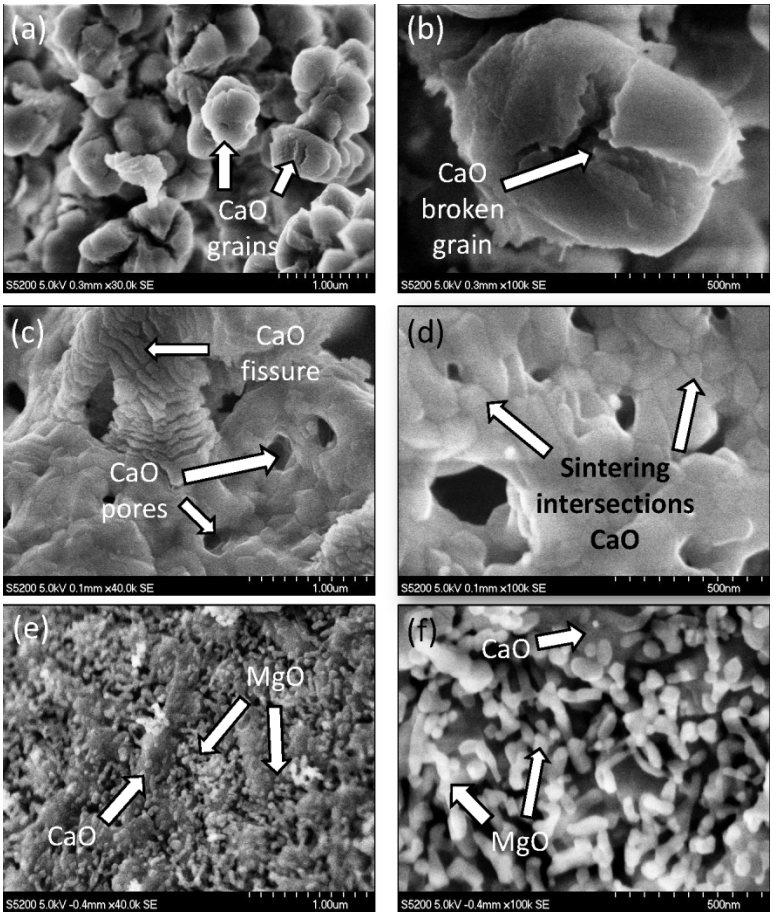


**Fig.9.** SEM micrographs of limestone after 20 cycles consisting of 5 min carbonation at 650ºC (15% $CO_2$/85% air vol/vol) and 5 min calcination at 950ºC (a and b) and 900ºC (c and d) (70% $CO_2$/30% air vol/vol), and micrographs of cycled dolomite at the same carbonation conditions but calcined at 900ºC (70% $CO_2$/30% air vol/vol) (e and f).

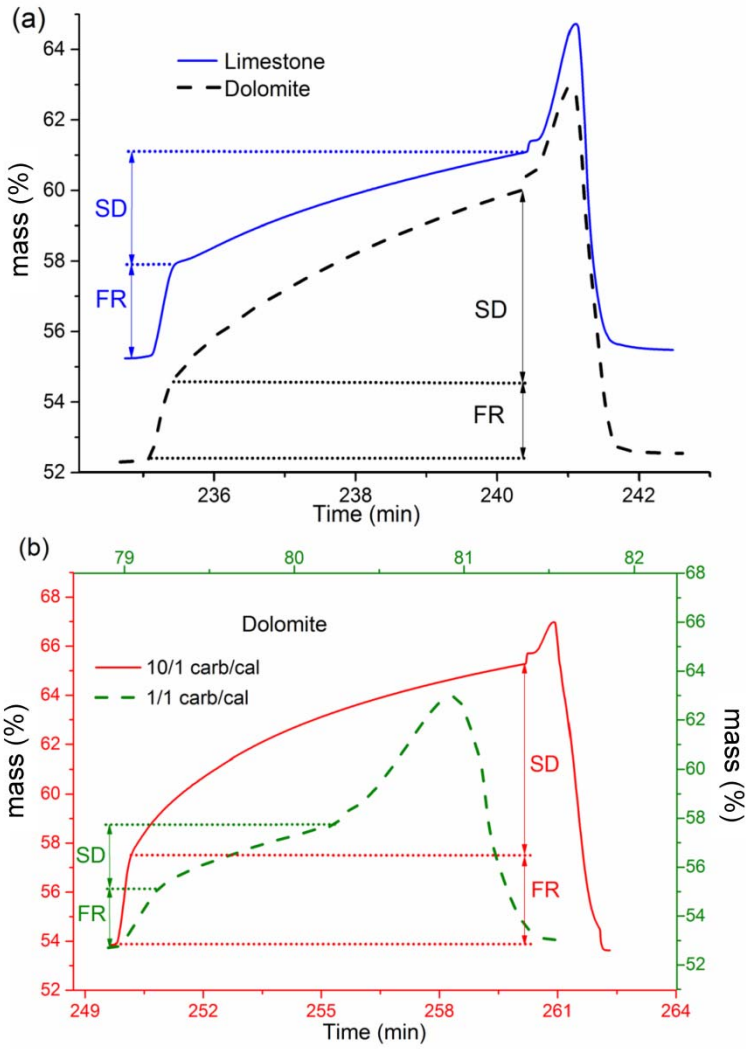


**Fig.10.** (a) Time evolution of the sorbent mass% during 5 minutes carbonation and calcination stages at the 20$^{th}$ cycle for natural dolomite and limestone. (b) Time evolution of dolomite mass% at the 20$^{th}$ cycle for residence times 10'/1' and 1'/1' carb/cal. Carbonation at 650ºC (15% $CO_2$/85% air vol/vol) and calcination at 900ºC (70% $CO_2$/30% air vol/vol). The two stages of carbonation (fast reaction-controlled FR and solid-state diffusion controlled SD) are indicated. The overshoot after the SD phase is due to a recarbonation in the transitory short period between the end of carbonation and calcination.

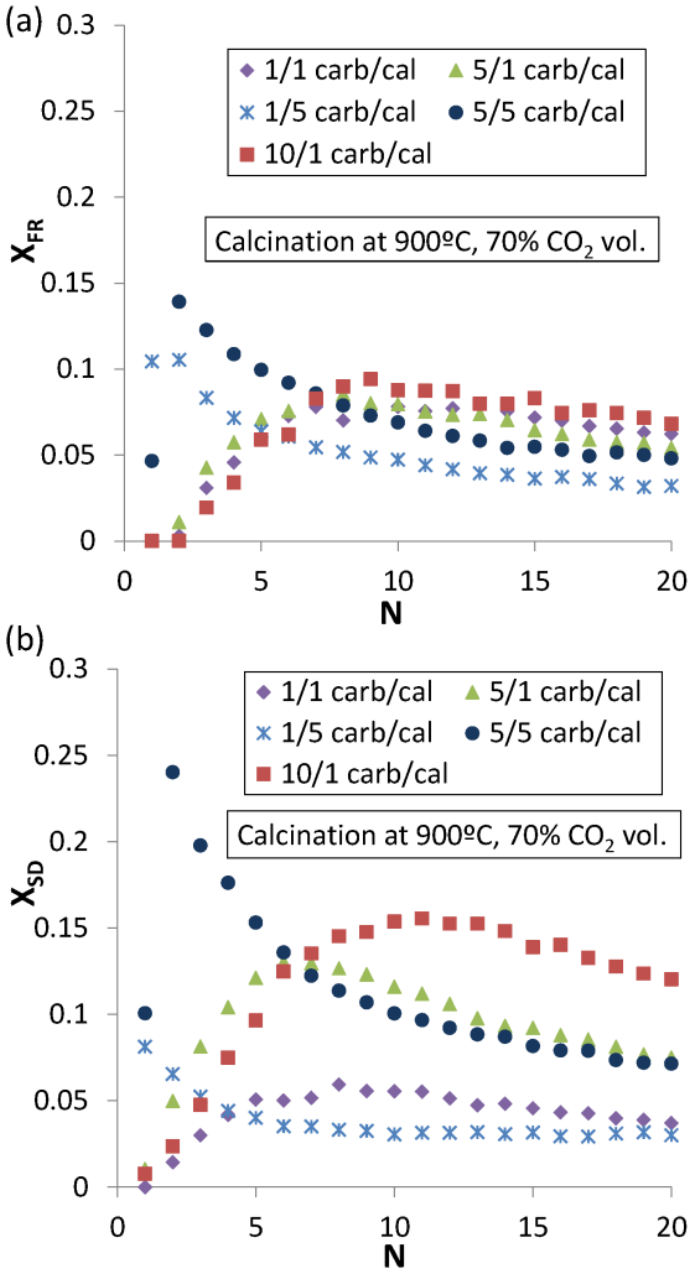


**Fig.11.** Conversion in the fast reaction controlled phase (a) and in the solid-state diffusion controlled phase (b) versus the cycle number for limestone. Calcination was carried out at 900ºC (70% $CO_2$/30% air vol/vol) for 1 and 5 minutes and carbonation at 650ºC (15% $CO_2$/85% air vol/vol) for 1, 5 and 10 minutes as indicated.

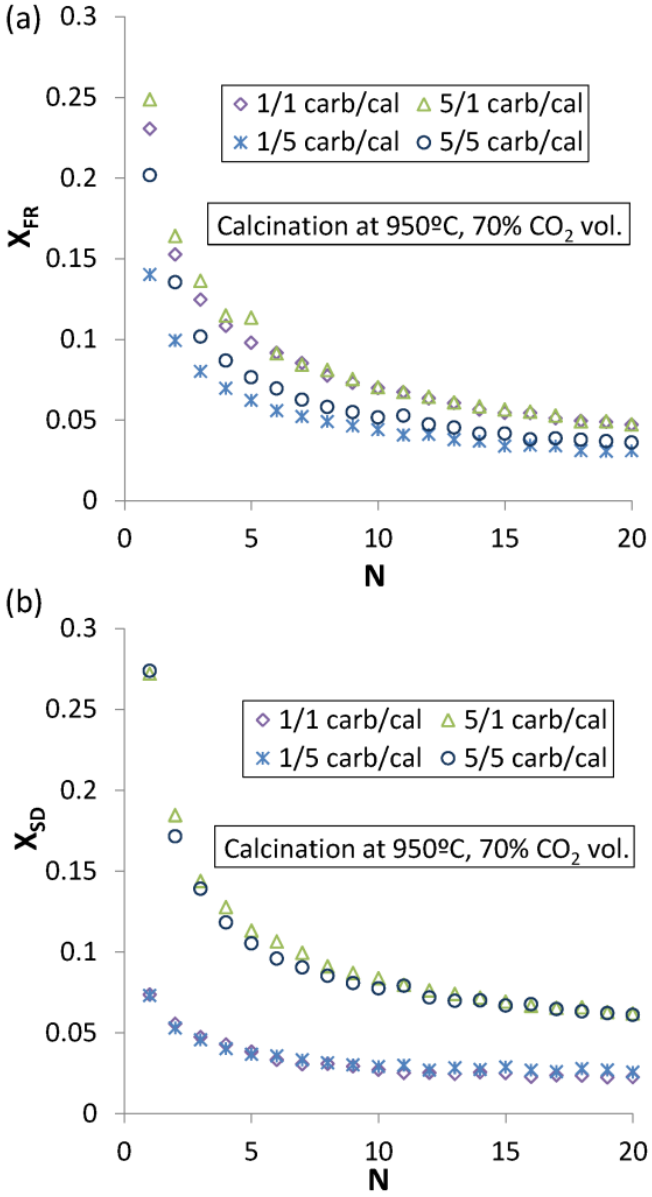


**Fig.12.** Conversion in the fast phase (a) and in the solid-state diffusion phase (b) versus the cycle number for limestone. Calcination at 950ºC (70% $CO_2$/30% air vol/vol) for 1 and 5 minutes and carbonation at 650ºC (15% $CO_2$/85% air vol.) for 1 and 5 minutes.

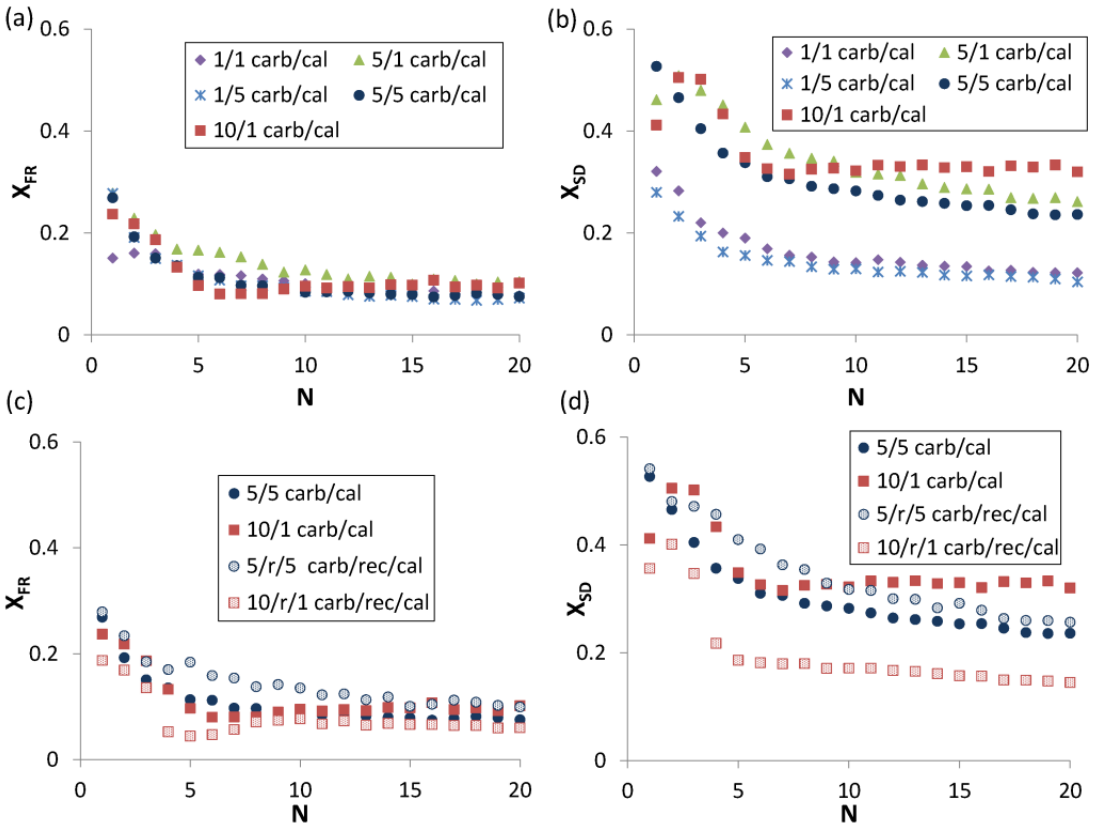


**Fig.13.** Conversion in the fast reaction-controlled phase (a and c) and in the solid-state diffusion phase (b and d) versus the cycle number for dolomite. Calcination at 900ºC (70% $CO_2$/30% air vol/vol) for 1 and 5 minutes, carbonation at 650ºC (15% $CO_2$/85% air vol/vol) for 1, 5 and 10 minutes, and recarbonation at 800ºC (90% $CO_2$/10% air vol/vol) for 3 minutes as indicated.

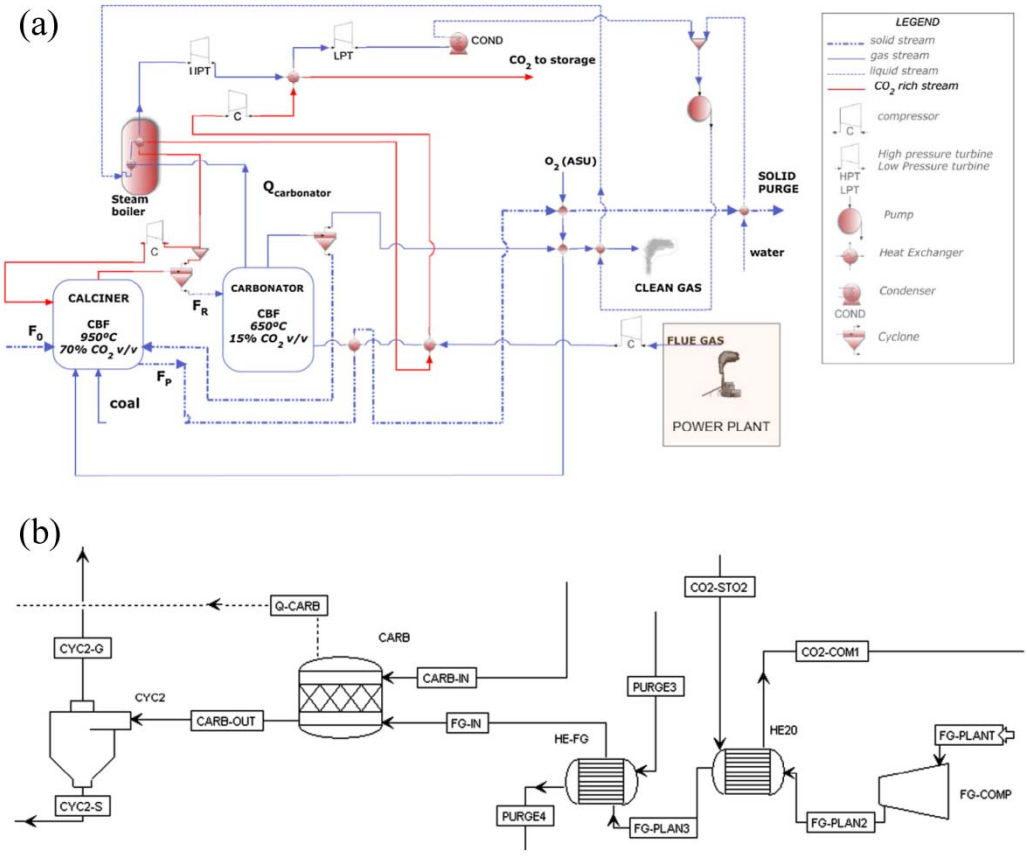


**Fig.14.** (a) General CFPP-CaL integration scheme. (b) Schematic representation of the carbonator zone used in the simulations. Reproduced with permission from Ref. [56]. $F_O$ is the mole flow of fresh makeup limestone (mol/s), $F_P$ is the mole flow of fresh makeup limestone (mol/s), $F_R$ is the mole flow of $CO_2$ in flue gas entering the carbonator, ASU is the air separation unit, FG-COMP is the flue gas compressor, FG-PLANT is the flue gas exiting the coal power plant, FG-PLAN2 is the compressed flue gas, HE20 is the gas-gas heat exchanger, CO2-COM1 is the $CO_2$ stream exiting the HE-FG equipment, HE-FG is the gas-solid heat exchanger, FG-PLAN3 is the flue gas entering into the HE-FG equipment, PURGE-i is the purge stream flow, CO2-STO2 is the $CO_2$ stream entering into the HE20 equipment, FG-IN is the flue gas entering into the carbonator, CARB is the carbonator reactor, CARB-IN are the solids entering into the carbonator, Q-CARB is the total heat produced in the carbonator, CARB-OUT is the stream exiting the carbonator, CYC2 is the cyclone linked to carbonator, CYC2-S is the solid stream exiting the CYC2 equipment, and CYC2-G is the gas stream exiting the CYC2 equipment.

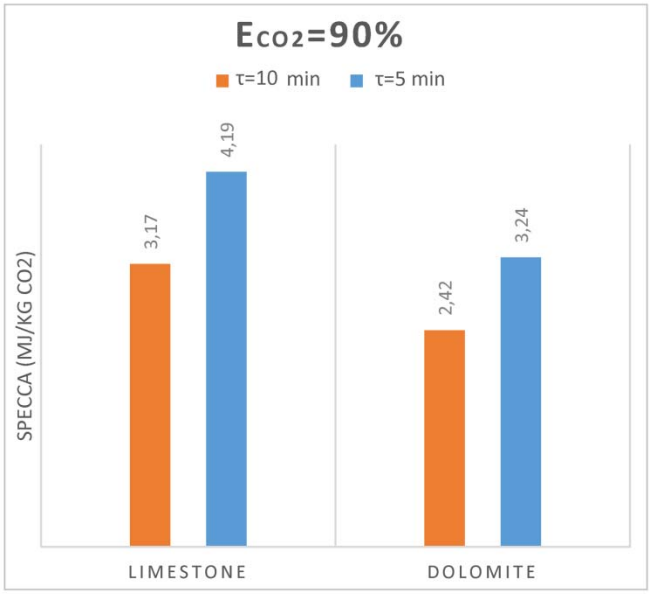


**Fig.15.** Energy required per kg of $CO_2$ captured obtained from the integration model of the CaL process into a 505 MWe coal fired power plant (Fig. 14), and using the TGA experimental results for limestone and dolomite shown in the present manuscript, as a function of solids residence time in the carbonator reactor (τ). Calculations are made by varying the ratio of fresh limestone makeup flow rate to $CO_2$ flow rate ($F_0/F_{CO2}$) to get a fixed $CO_2$ capture efficiency ($E_{CO2}$) value of 90% (see [56] for further details).